Progress in Organic Coatings 90 (2016) 258–266

Contents lists available at ScienceDirect

Progress in Organic Coatings

journal homepage: www.elsevier.com/locate/porgcoat

Environmentally friendly assembly multilayer coating for flame retardant and antimicrobial cotton fabric

Fei Fang[a,b,1], Xiaoxuan Chen[b,1], Xian Zhang[b,*], Cheng Cheng[a], Dezhi Xiao[a], Yuedong Meng[a], Xin Ding[b], Hui Zhang[c], Xingyou Tian[b,*]

[a] Institute of Plasma Physics, Chinese Academy of Sciences, Hefei 230031, People's Republic of China
[b] Institute of Applied Technology, Hefei institutes of Physical Science, Chinese Academy of Sciences, Hefei 230031, People's Republic of China
[c] School of Physics and Materials Science, Anhui University, Hefei 230039, People's Republic of China

ARTICLE INFO

Article history:
Received 27 September 2015
Accepted 29 September 2015
Available online 15 November 2015

Keywords:
Cotton fabric
Environmentally friendly
Flame retardant
Antimicrobial
LBL assembly coating

ABSTRACT

Potassium alginate (PA), a green polymeric material extracted from seaweed, was firstly coupled with environmentally friendly antimicrobial polyhexamethylene guanidine phosphate (PHMGP) to build flame retardant and antimicrobial coating on cotton fabric via layer-by-layer (LBL) technique. Attenuated total reflectance infrared spectroscopy analysis shows that PHMGP and PA grow linearly in LBL deposition process. Thermogravimetric analysis results indicate that the coated fabric leaves higher residue char than the uncoated after testing, owing to the char former feature of the assembly coating. Microcombustion tests show that the peak heat release rate and total heat release of fabric sample are decreased after coated with PHMGP-PA coating. The results of flammability tests reveal that the afterglow phenomenon was effectively eliminated by the PHMGP-PA coating. Scanning electron microscope and infrared spectroscopy results confirm that the assembly coating exerts useful intumescent flame retardant effect on cotton fabric. Furthermore, antimicrobial qualitative assessment reveals that the fabric coated with increased bilayers performs an improved antimicrobial effect on *Escherichia coli* (*E. coli*). The quantitative determination results show that the coated fabric can inactivate 100% *E. coli* and *Staphylococcus aureus* in 5 and 30 min, respectively.

1. Introduction

Cotton, one of the most abundant natural celluloses, has been widely applied in clothing, home textiles and industrial goods [1]. However, to further extend its application in some special scenarios, researchers have paid more and more attention to the functional modifications on cotton fabric. Through surface grafting or coating with functional materials, cotton was imparted various properties such as flame retardation [2,3], UV resistance [4,5], antimicrobial [6,7], and super-hydrophobic [8,9].

In recent years, layer-by-layer (LBL) technique, a promising method capable of imparting versatility on various substrates [10–12], has been widely applied on the functional modifications of cotton [13,14]. This technique was firstly suggested by Iler [15], largely developed by Decher [16] and further established as a simple and inexpensive approach for material surface modification. Multifarious potential functions such as flame retardant [17], antimicrobial [18], and super-hydrophobic [19], have been exploited on the assembled multilayer film by alternating deposition of positive and negative charged materials.

It is noteworthy that, to overcome cotton's shortcoming of flammability, LBL assembly technique has been introduced to assemble flame retardant coating on cotton fabric. This technique was firstly applied in cotton fabric in 2009 by depositing polyelectrolyte/nanosilicate inorganic LBL flame retardant coating, which could effectively improve the thermal stability of cotton [20]. Afterwards, various inorganic nanoplatelets or nanoparticles including montmorillonite [17,21], alpha-zirconium phosphate [22], polyhedral oligomeric silsesquioxane [23] and colloidal silica [24] were used to the LBL flame retardant treatment of textile fabrics by creating thermal shield layer on the fabric surface. Significantly, a more efficient flame retardant system, organic intumescent coating, was constructed on cotton in 2011 by alternately depositing anionic poly(sodiumphosphate) (PSP) and cationic poly(allylamine) (PAAm) [25]. 20 bilayer (BL) PSP/PAAm assembly coating could completely extinguish the flame on

* Corresponding authors. Tel.: +86 551 65591418; fax: +86 551 65591434.
E-mail addresses: xzhang@issp.ac.cn (X. Zhang), xytian@issp.ac.cn (X. Tian).
[1] These authors contributed equally to this work and should be considered co-first authors.

http://dx.doi.org/10.1016/j.porgcoat.2015.09.025
0300-9440/

cotton fabric during burning. As we known, the high flame retardant efficiency of the intumescent coating was attributed to the strong combination of blowing agent, acid and carbon sources [26]. When exposed to the fire, the assembly coating favored the formation of intumescent char that served as a thermal insulating layer and shielded the internal cellulose from outside heat and oxygen. Subsequently, the intumescent coatings with various combinations were constructed on textile fabrics for effective flame retardant treatment by employing intumescent components including cationic chitosan (CH) [27], polyethylenimine [28,29], and starch [30], and anionic ammonium polyphosphate (APP) [31], phytic acid [32] and deoxyribonucleic acid (DNA) [33], PSP [34], phosphorylated cellulose [35], poly(vinylphosphonic acid) [36], poly(phosphoric acid), phosphorylated chitin [37].

Apart from the inherent defect of flammability, cotton fiber has porous and hydrophilic structure, which encourages the growth of bacteria [38]. The thriving bacteria may cause diseases in humans and produce acidic compound that will catalyze the degradation of cellulose [39]. Therefore, it is highly desirable to prepare flame retardant and antimicrobial multifunctional cotton fabric. In our prior work, multifunctional cotton with flame retardant and antimicrobial properties has been developed by introducing polyhexamethylene guanidine phosphate (PHMGP) into assembly coating [40]. This coating performed effective inhibitory action on the growth of *Escherichia coli* (*E. coli*) and *Staphylococcus aureus* (*S. aureus*). Except for antimicrobial performance, strong intumescent flame retardant effect on the cotton was also achieved by the cooperation of PHMGP with APP.

It is of great concern that there may be some toxicity and environmental problems with various functional treatments on textiles such as clothing and household articles that come in close contact with skin. In view of that, researchers have started to distract their attention on flame-retardant textile using green and renewable materials such as CH, phytic acid [32], DNA [33,41], caseins [42], starch [30], and cellulose and chitin derivatives [35,37]. Hence, it is favorable to use some environmentally friendly materials for the multifunctional treatment on textiles. Remarkably, PHMGP can theoretically perform intumescent flame retardant effect, because of its richness of nitrogen and phosphorus elements. Even as a synthetic antimicrobial, it is environmentally friendly, biodegradable and nonirritant [43]. Moreover, polyhexamethylene guanidine salts have been extensively used as disinfectors in food production [44], healthcare industry [45] and aquatic agriculture [46,47]. Potassium alginate (PA) is a carbon-rich molecule that can be assembled with PHMGP to compose a completely intumescent system. As an anionic polyelectrolyte, it can be alternately deposited with cationic PHMGP in LBL assembly coating. Importantly, alginate is a green material extracted from seaweed [48], which is a kind of extremely abundant biodegradable and biocompatible natural resource. The natural environmental protection feature has led to its extensive use in food industry [49,50], biomedical [51,52] and cosmetic fields [53]. Additionally, some divalent alginates have been identified as intrinsic flame retardant materials by generating stable carbonaceous char during burning [54,55]. To the best of our knowledge, although some renewable flame retardant coatings have been introduced into cotton fabric, there are few reports on environmentally friendly multifunctional assembly coating with flame retardant and antimicrobial properties.

In the present work, environmentally friendly and biodegradable PHMGP-PA assembly multilayer was constructed on cotton fabric to achieve flame retardant and antimicrobial performances. Attenuated total reflectance Fourier transform infrared (ATR-FTIR) spectroscopy analysis was conducted to detect the growth of PHMGP-PA coating in the process of LBL deposition. Thermogravimetric analysis (TGA) and by microcombustion calorimetry (MCC) were carried out to monitor the thermal decomposition of fabric samples. The flame retardant properties were estimated by flammability test in both vertical and horizontal direction. The antimicrobial action was assessed by Kirby-Bauer test and a modified AATCC test method 100-2004.

2. Experimental

2.1. Materials

PHMGP solution (polymeric level >60, 25 wt%) was supplied by Shanghai Scunder Industry Co., Ltd. PA solution (300–800 mpa s, 1 wt%) was purchased from Qingdao Bright Moon Group Co., Ltd. Cotton textile (230 g/m^2) was obtained by an online textile shop. All materials were used without treatment.

2.2. LBL deposition

0.1 wt% PHMGP and 0.1 wt% PA aqueous solutions were used as the cationic and anionic deposition solutions, respectively.

Before the LBL assembly, cotton fabric was dipped in deionized water for one day, and then it was further dried at 60 °C for 40 min. Cotton fabric was tandem dipped in cationic PHMGP deposition solution and anionic PA solution for 5 min, as a primer BL. In this process, cationic PHMGP was initially deposited because there exhibits the electrostatic linking between PHMGP and the anionic carboxylate groups on cotton. Then, the cotton was alternately immersed into the cationic and anionic solution for 1 min until the desired number of BL (5, 10 and 20) was obtained. After each immersion, the sample was washed with deionized water for 1 min and dried at 60 °C for 40 min. The final add-ons of the 5, 10 and 20 BL coated fabrics relative to the uncoated fabric were 1.1, 2.0 and 4.8 wt%, respectively, as listed in Table 1.

2.3. Characterization

ATR-FTIR spectra of the fabric samples were obtained by an infrared spectrometer (32 scans and 4 cm^{-1} resolution, Thermo Nicolet Corporation, USA). This spectrograph is provided with a Ge crystal. FTIR spectra of their residual chars after VFT were also recorded by a Nicolet infrared spectrometer.

Thermal-oxidative decomposition of the fabric samples was monitored by a Pyris 1 thermo gravimetric analysis (TGA) (PerkinElmer, USA). The samples were heated form 50 to 600 °C at the rate of 10 °C /min in air atmosphere.

The combustion behaviors of the fabric samples were investigated by a FAA Microscale Combustion Calorimeter (FTT limited, USA). All fabric samples were analyzed from 50 to 600 °C at the heating rate of 1 °C/s. In addition, the oxygen and nitrogen flow rates were 80 mL/min and 20 mL/min, respectively.

Vertical flammability test (VFT) and horizontal flammability test (HFT) was carried out on an AG5100A Horizontal Vertical flame tester (Zhuhai Angui Testing Instrument Co., Ltd) according to ASTM D6413 and D5132, respectively.

The fabrics samples and residual chars were photographed by a Sirion 200 field emission scanning electron microscope (SEM) (FEI Corporation, USA); an energy-dispersive X-ray (EDX) spectrometer was used to conduct elemental analysis (beam voltage: 10 kV).

The antimicrobial performances of the fabric samples were qualitatively assessed against *E. coli* by the Kirby-Bauer test described by Fang et al. [40]. The number of inhibited colony was calculated by Eq. (1):

$$\text{Inhibited Colony number} = \frac{(r^2 - 64)}{R^2} \times \text{CFU}$$

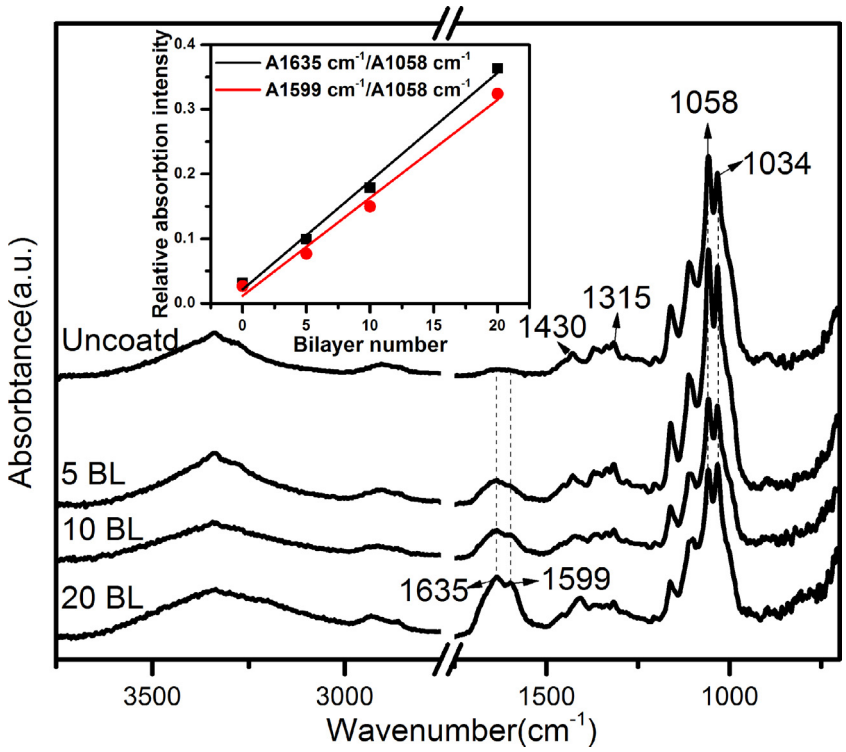

Fig. 1. ATR-FTIR spectra of the cotton fabrics samples. The inset shows the relative intensity ratios of N–H/C–O–C and COO–/C–O–C.

where r is the diameter of the zone of inhibition (ZOI), R is the diameter of the bacterial growth area, and CFU represents colony forming unit.

The antimicrobial effects of the fabric samples were quantitatively tested against *E. coli* and *S. aureus* by using a modified AATCC Test Method 100-204. This method was designed for the dissolving type antimicrobial fabric. Fabric swatches with 10 mm × 10 mm were inoculated with 100 μL of 1.7×10^5 *E. coli* or 1.6×10^5 CFU/mL *S. aureus* in sealed and sterile petri dishes. All samples were incubated at 37 °C for 5 or 30 min and then added into 10 mL sterile water. Afterwards, the samples were ultrasonic treated and vortexed for 1 min, respectively. Serial dilutions of these samples were deposited on tryptose agar and cultivated at 37 °C for 24 h. Finally, bacterial reduction was calculated by the following Eq. (2):

$$\text{Bacterial reduction} = \frac{(U_t - C_t)}{C_t} \times 100\% \quad (2)$$

where U_t and C_t are the surviving bacterial colonies (CFU/mL) for the fabric samples, respectively.

3. Results and discussion

3.1. FTIR analysis

The coatings of the fabric samples were assessed by ATR-FTIR spectroscopy (see Fig. 1). The virgin cotton presents the characteristic peaks of cellulose at 1430, 1374, 1315 and 1058 cm^{-1}, which are ascribed to the C–H in-plane bending, deformation stretching, wagging and C–O–C asymmetry stretching [56], respectively. Due to the similar structure with cellulose, PA shows overlapping absorption peaks with cotton among 1034–1163 cm^{-1}, belonging to C–O–C stretching. The presence of PA on the coated fabrics can be confirmed by the appearance of the signal at 1599 cm^{-1}, which is ascribed to antisymmetric COO– stretching vibration [57]. Compared to the uncoated cotton, the coated samples show a new signal at 1635 cm^{-1}, ascribing to the N–H bending of PHMGP [58]. The intensities of the peaks at 1635 and 1599 cm^{-1} are strengthened gradually with the growth of PHMGP-PA BL.

To further analyze the PHMGP-PA coating growth, the absorption value at 1058 cm^{-1} (C–O–C stretching vibration) is used as the reference. The relative intensity ratios (N–H/C–O–C: A1635 cm^{-1}/A1058 cm^{-1}, COO–/C–O–C: A1599 cm^{-1}/A1058 cm^{-1}) are calculated as the representatives of BL number of the PHMGP-PA coating. As shown in inset, the relative intensity ratios (A1635 cm^{-1}/A1058 cm^{-1} and A1599 cm^{-1}/A1058 cm^{-1}) increase linearly with the number of BL, confirming that the PHMGP and PA amounts increase linearly in whole LBL process.

3.2. Thermal stability

The thermal-oxidative decomposition processes of the fabric samples were investigated by TGA. Pure cotton fabric starts to break down at 317 °C ($T_{-5\%}$) and is dehydrated to form aliphatic compounds [59]. In the first decomposition stage (200–400 °C), it shows the maximum weight loss rate at 362.6 °C (T_{max1}). During the second decomposition stage (400–600 °C), the aliphatic compounds are further carbonized into graphitized char and simultaneously oxidized to generate volatile gases CO_2 and CO.

By introducing the PHMGP-PA coating, the 5 BL and 10 BL coated fabrics show increased initial degradation temperatures ($T_{-5\%}$) with respect to pure cotton, as listed in Table 1, indicating an enhanced thermal stability of cotton fabric after the LBL assembly process. However, as the BL number increases to 20, the $T_{-5\%}$ anomalously decreases to 285 °C due to the more obvious decomposition of PA, which involves the destruction of glycosidic bonds [60]. As shown in Fig. 2(a) and (b), PA decomposes rapidly at 257 °C to form some decomposition products, which have high thermal stability below 500 °C and provide a protective layer for cotton. As a consequence, the coated samples show increased T_{max1}, suggesting that cotton's thermal decomposition process is delayed under the protection of the decomposition products. Furthermore, thanks

Table 1
TGA data of pure PHMGP, PA and cotton and coated fabrics in air.

Sample	Add-on (wt%)	$T_{-5\%}$ (°C)	T_{max1} (°C)	T_{max2} (°C)	Residue at 500 °C (wt%)	Residue at 600 °C (wt%)
Uncoated		317	363	482	7.3	3.9
5 BL	1.1	328	386	–	15.8	8.2
10 BL	2.0	331	377	–	20.6	11.9
20 BL	4.8	285	373	–	24.2	12.7
PA		229	257	526		29.8
PHMGP		148	385	464		14.6

to the protective effect, cotton shows synchronous decomposition process with PHMGP in the initial stage. In this case, the released phosphoric acids from PHMGP can accelerate the thermal degradation of cotton. This can be verified by the higher weight loss rate at T_{max1}, as shown in Fig. 2(c). Meanwhile, the phosphoric acids also catalyze the formation of graphitized char, as a protective layer, which will inhibit the further decomposition of cotton in higher temperature. As a consequence, the second decomposition peaks disappear in the TGA curves of the coated fabrics, further confirming the formation of highly stable carbon structure. Additionally, the catalytic charring of PHMGP can also be confirmed by the increased residues of the coated fabrics at 500 and 600 °C (see Table 1). Furthermore, the residue char increases with the growth of the BL number and the final residues left are significantly higher than the add-ons, as listed in Table 1, indicating a substantial part of fabric has been transformed into thermally stable char in the presence of PHMGP-PA multilayer during burning. These results indicate that the PMGP-PA assemblies perform useful flame retardant effect on cotton fabric by promoting the thermostable char formation.

In order to verify the char forming effect of the PHMGP-PA coating, the combustion behaviors of the fabric samples were monitored by MCC. The HRR curves were reported in Fig. 3 and the calculated data were collected in Table 2. During testing, cotton is pyrolyzed in nitrogen and the generated volatiles are further combusted in the presence of oxygen. In MCC, cotton begins to degrade at 322 °C (T_{onset}) and presents the peak heat release rate (PHRR) at 375 °C (T_p) that are higher than the $T_{-5\%}$ and T_{max1} in TGA, respectively. It can be observed that cotton's pyrolysis in nitrogen lags behind its thermo-oxidative degradation in air. In this instance, cotton's pyrolysis synchronizes with that of PHMGP. As shown in Fig. 3, the coated fabrics show lower $T_{-5\%}$ and T_p values as compared to the uncoated sample, as a result of the catalyzed thermal degradation of cotton fabric caused by PHMGP. Furthermore, the released phosphoric acids from PHMGP could further favor the char formation and impede the volatiles release. As a consequence, the coated fabrics exhibit reduced values of PHRR and total heat release (THR) (see Table 2). Additionally, the PHRR and THR values decrease with the BL number, suggesting that the char forming effect increases with the growth of BL number. As the BL number increases to

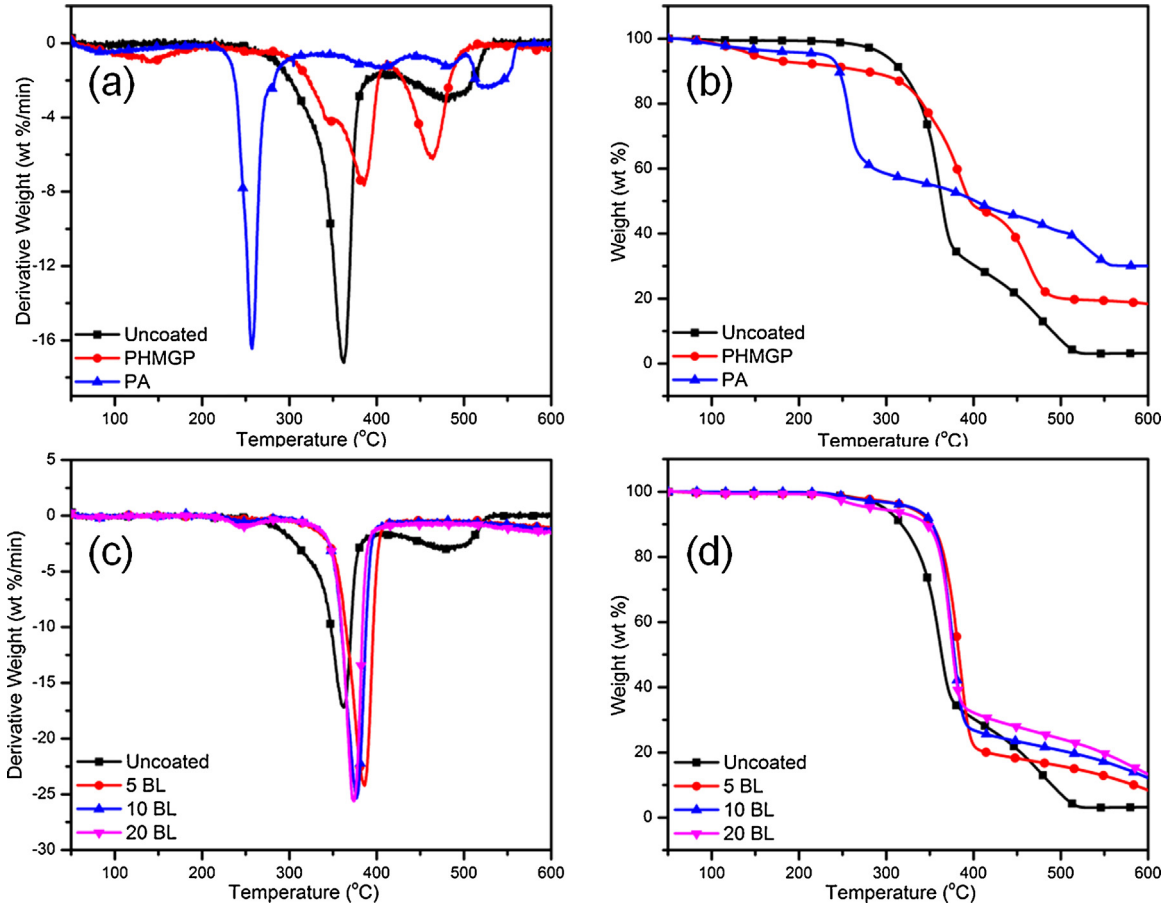

Fig. 2. DTG and TG curves of pure PHMGP, PA and cotton (a and b) and the fabrics samples (c and d).

Table 2
MCC data of the fabric samples.

Sample	T_{onset} (°C)	PHRR (W/g)	T_p (°C)	THR (kJ/g)
Uncoated	322	260	375	13.5
5 BL	303	207	360	11.1
10 BL	289	190	356	10.9
20 BL	302	184	357	10.3

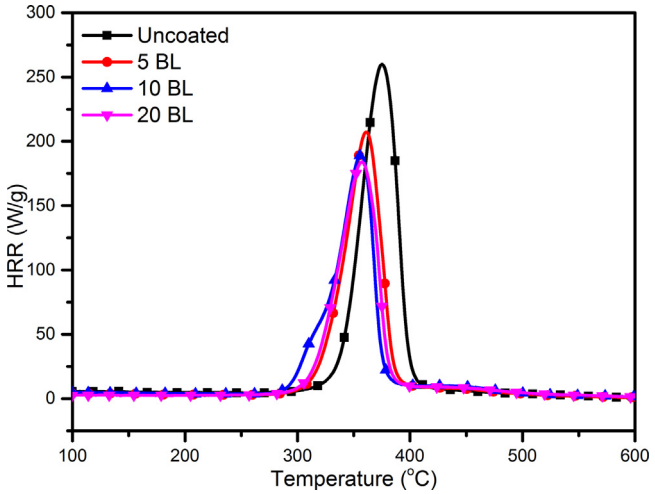

Fig. 3. MCC curves of the fabric samples.

20, the PHRR and THR values decrease to 184 W/g and 10.3 kJ/g, reduced by 29% and 24%, respectively. These results confirm that the PHMGP-PA coating facilitates the char formation and prevents the generation of volatiles during combustion.

3.3. Flame retardant property

The flame resistances of the fabric samples were assessed by VFT. The uncoated cotton burns with vigorous flame after direct exposure to heat source. After extinguishing, there appears 14 s afterglow and then cotton is almost completely burned up without any remains left. After the introduction of the PHMGP-PA coating, the coated fabrics show similar after-flame time with the uncoated cotton, as listed in Table 3. Even so, the PHMGP-PA assembly coating can effectively eliminate the afterglow phenomenon, as shown in Fig. 4 at 2 s after extinguishing. After VFT, the coated fabrics still leave considerable residue char (see Figs. 4 and 5) and the mass of the residue left increases with the increasing BL number. With only 1.1 wt% coating on fabric, 5 BL leaves 2.7 wt% residue char after burning. For the 10 BL coated fabric (2.0 wt%), 3.2 wt% residue char is left after VFT. As the BL number grows to 20 (4.8 wt%), the residue char increases to 5.5 wt%. Although no abundant residues are left in the coated fabrics after VFT, the higher mass of the residues with respect to that of coatings further suggest that the PHMGP-PA coating promotes the formation of thermally stable char during burning.

The combustion behaviors of the fabric samples were further monitored by HFT. The virgin cotton burns for 174 s (burning rate 1.47 mm/s) and consumes completely after testing. After the deposition of the PHMGP-PA coating, the burning time decreases to 137, 140 and 147 s for the 5, 10 and 20 BL coated samples, respectively. It can be seen that the deposition of the assembly coating increases the burning rate of cotton fabric during HFT. However, the burning rate decreases with the growth of BL number, from 1.86 mm/s (5 BL) to 1.74 mm/s (20 BL), as a result of the enhanced flame retardant effect of the coating with increased BLs. No residue char is left from the uncoated fabric after HFT, and substantial residue chars are left in the coated fabrics (see Figs. 4 and 5). Moreover, the residue mass increases with the growth of the LBL coating, similar with the results in VFT.

To investigate the fire-retardant mechanism of the PHMGP-PA coating, the fabric samples and their residues after burning were observed by SEM. Virgin cotton fiber presents a smooth surface (see Fig. 6). After LBL assembly process, the PHMGP-PA multilayer film is evenly coated on the fiber surface. No obvious adhesion phenomenon appears in all coated fabrics, and as is expected, these fabrics still maintain their high softness. Although all coated fabrics are somewhat damaged, the wave structures are well-preserved after burning. At high magnification, it can be observed that the fibers shrink and curl for the 5 and 10 BL coated fabrics during burning. Remarkably, some intumescent bubbles appear on the fibers surface of the 20 BL coated fabric, as a result of the flame retardant coating reaction to the fire. EDX analysis result shows the presence of carbon, oxygen, phosphorus and potassium in the bubbles. The formation process of intumescent bubbles can be described

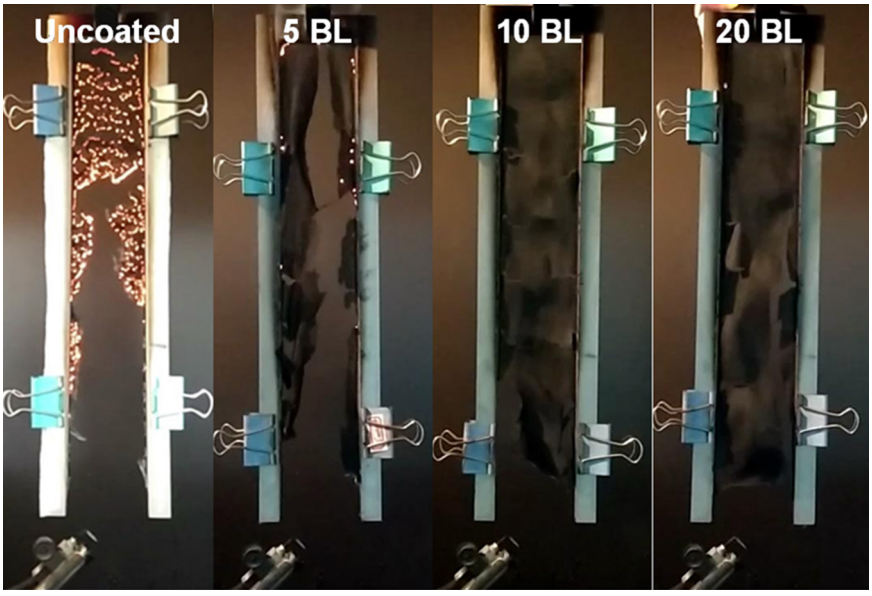

Fig. 4. Photographs of the fabric samples at 2 s after extinguishing during VFT.

Table 3
VFT and HFT data of the fabric samples.

Sample	Vertical				Horizontal	
	After-flame time (s)	Afterglow (s)	Residue (wt%)	Burning time (s)	Burning rate (mm/s)	Residue (wt%)
Uncoated	20	14	–	174	1.47	–
5 BL	20	0	2.7	137	1.86	3.4
10 BL	22	0	3.2	140	1.82	4.4
20 BL	20	0	5.5	147	1.74	5.8

as follows: the phosphoric acid released from PHMGP phosphorylates the cellulose and alginate, catalyzes the dehydration and carbonization reactions and then results in the formation of carbon and phosphorus-rich char, which is further expanded by the non-combustible gas released from PHMGP. Thus, the PHMGP-PA assembly coating exerts good intumescent flame retardant effect on cotton, in which PHMGP acts as both blowing agent and acid source.

The char residues of the coated fabrics after VFT were further studied by FTIR analysis. All residues after burning show characteristic peaks of aromatic ring (skeletal vibration) at 1616, 1593 and 1451 cm^{-1} (see Fig. 7). Additionally, the presence of benzene

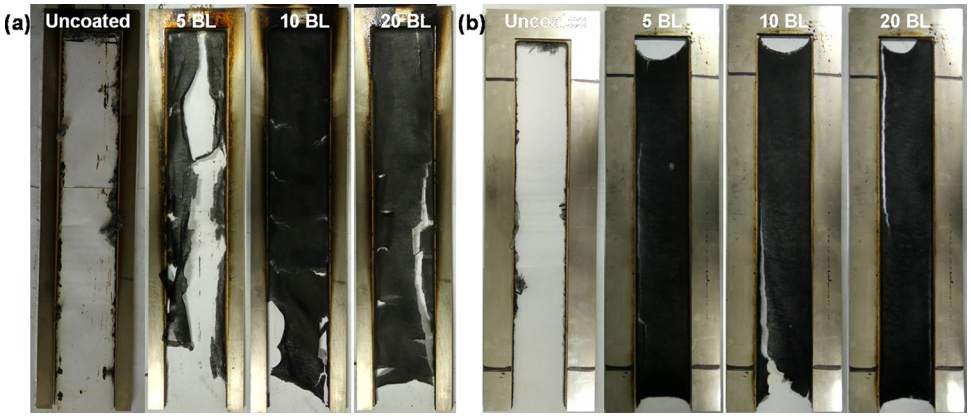

Fig. 5. Photographs of the residue chars of the fabric samples after VFT (a) and HFT (b).

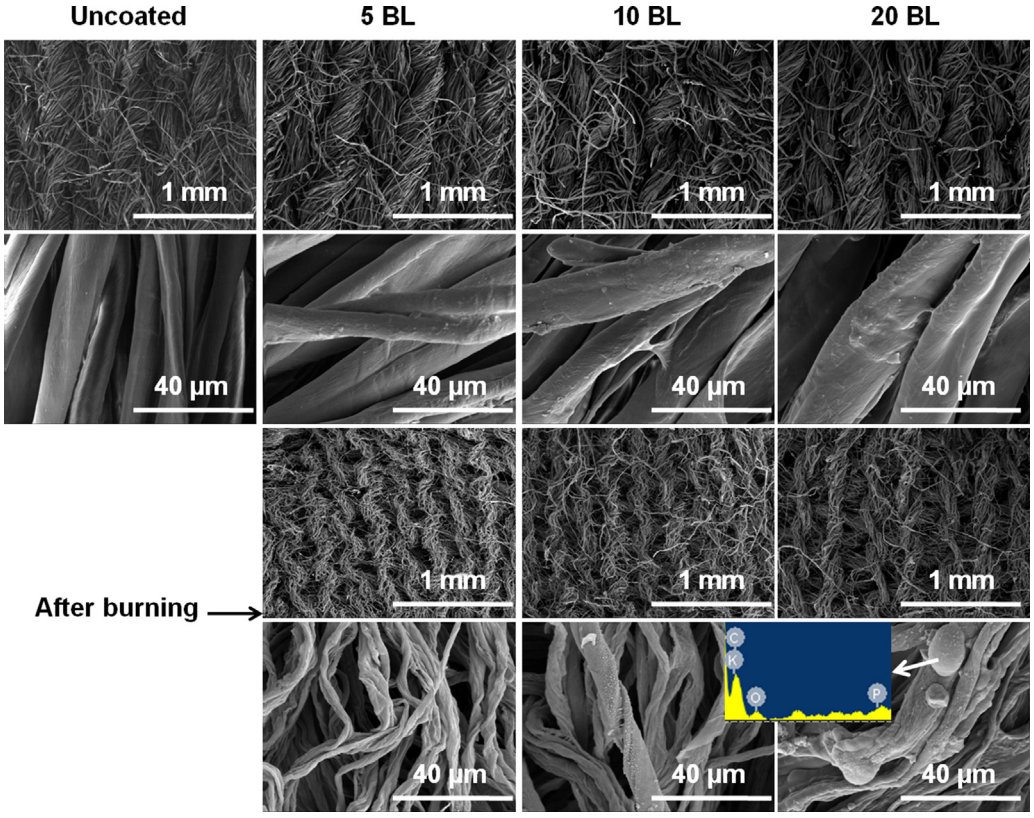

Fig. 6. SEM photographs of the fabric samples before and after burning.

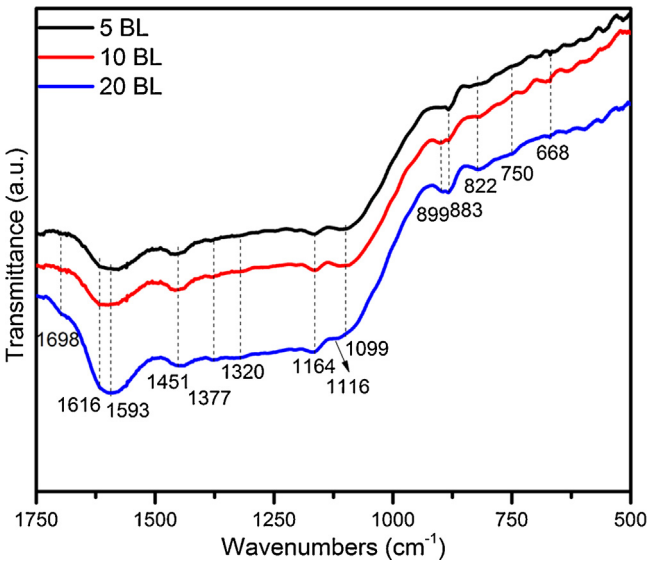

Fig. 7. FTIR spectra of the residues of the coated fabrics after burning.

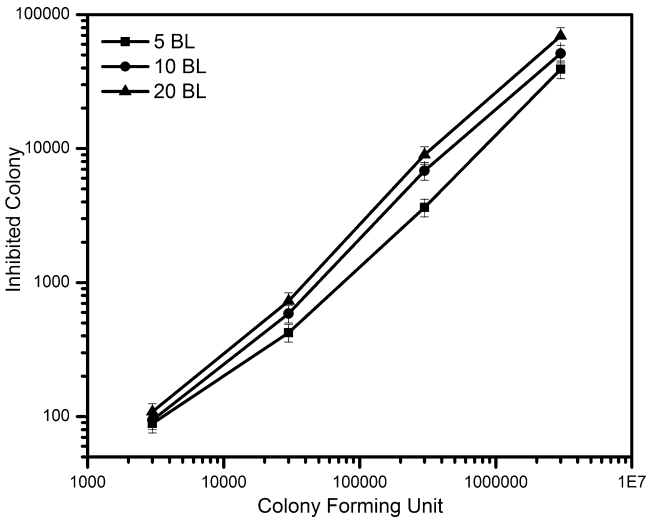

Fig. 9. Inhibited colony as a function of *E. coli* CFU for each coated fabrics. Error bars reflect 15% error range.

ring in the char can be further confirmed by the emergence of the absorption peaks at 899, 822 and 668 cm^{-1}, which are attributed to the out-of-plane vibrations of the aromatic compounds. The peaks at 1099 and 883 cm^{-1} can be assigned to the stretching vibrations of P–O–P [61], indicating that the formation of polyphosphoric acid. The 20 BL coated fabric shows a stronger absorption band between 1500 and 1680 cm^{-1} as compared to the 5 and 10 BL coated fabrics, indicating an enhanced aromatization effect with the increasing number of BL during burning. Moreover, the intensities of the peaks at 1377 and 750 cm^{-1} increase with the BL number, suggesting the formation of phosphorus-nitrogen structure during burning [62]. These results reveal that the PHMGP-PA coating promotes the formation of aromatic char with stable phosphorus-nitrogen containing structure during burning.

3.4. Antimicrobial properties

The antimicrobial actions of the coated fabrics on *E. coli* were firstly qualitatively measured by Kirby-Bauer test. The coated samples inhibit the growth of bacteria and exhibit an augmented ZOI with a decreased colony of *E. coli* (see Fig. 8). For example, the 10 BL sample presents a 12 mm ZOI at the colony of 3×10^3 CFU, and the ZOI is 11 mm at 3×10^5 and 3×10^4 CFU. As the colony increases to 3×10^6, the ZOI decreases to 10.5 mm. With the colony rises to 3×10^7, the ZOI will be approximate to the size of sample and hard to be measured accurately. Then, the inhibited colony number was further calculated by Eq. (1) in the Characterization. As shown in Fig. 9, the inhibited colony number grows approximately linearly on a log–log plot with the colony of bacteria. For example, 10 BL inhibits 90 CFU *E. coli* at the colony of 3×10^3 CFU, and the inhibited colony number increases to 600 and 7000 at the colony of 3×10^4

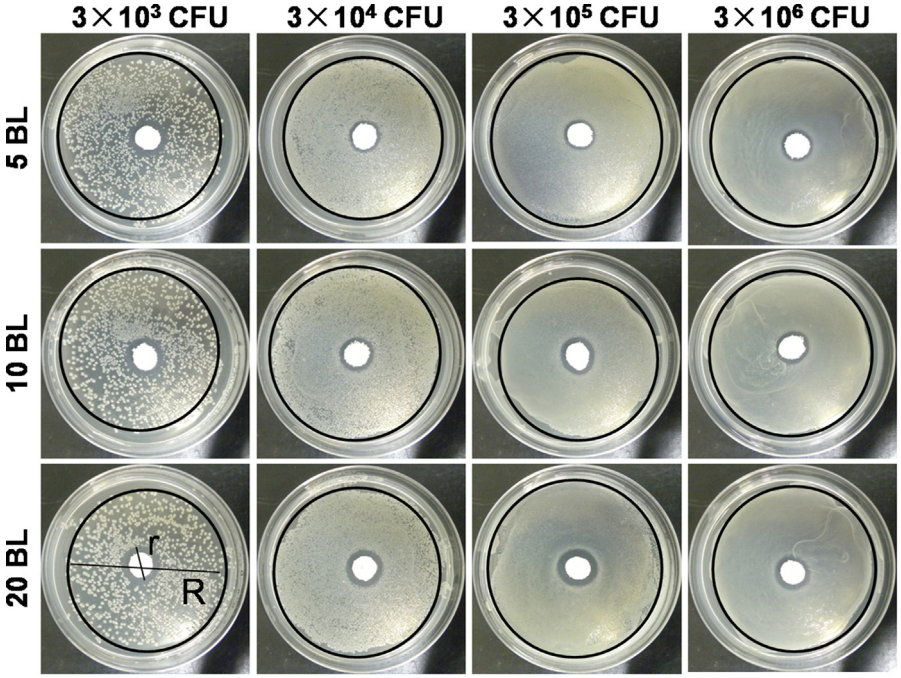

Fig. 8. The photographs of *E. coli* growth inhibition by the coated fabrics.

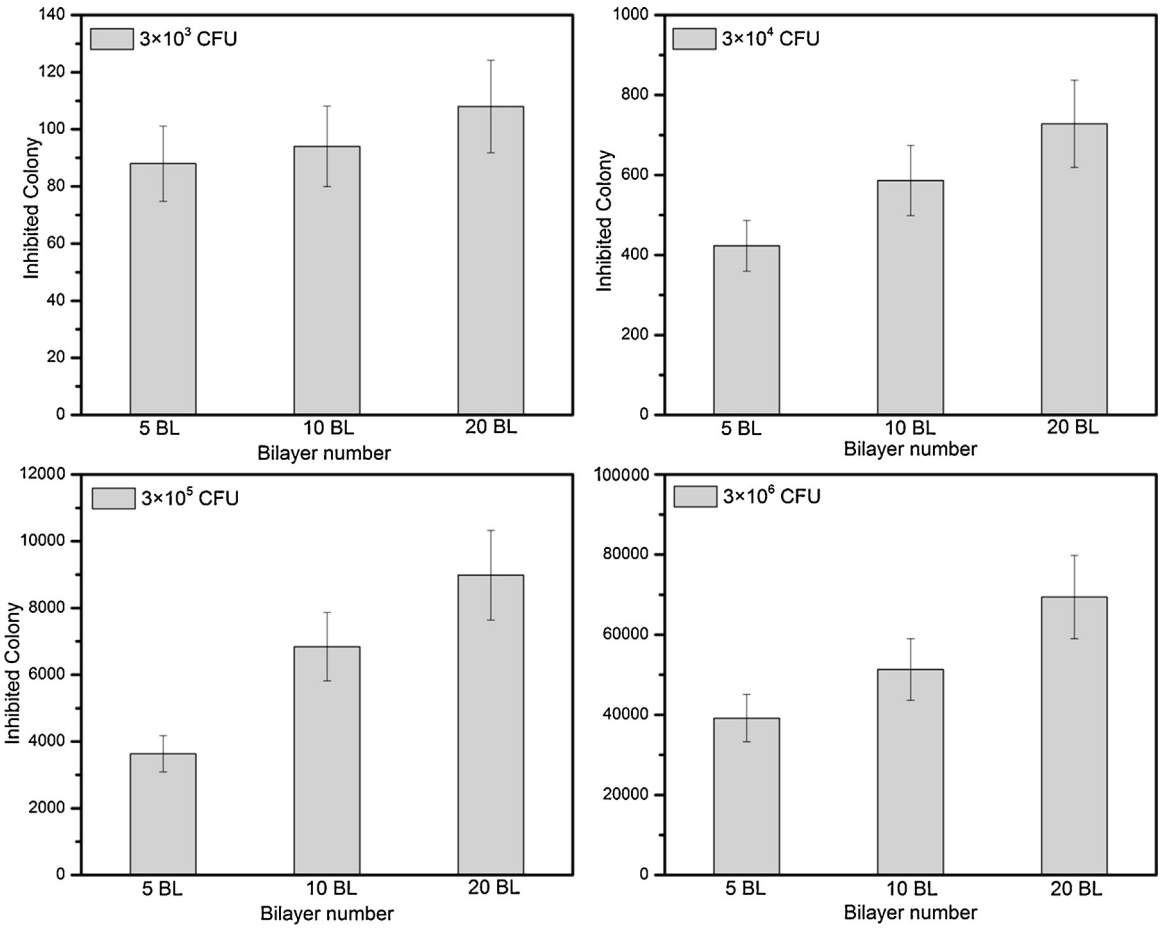

Fig. 10. Inhibited colony as a function of BL number in coatings for each *E. coli* CFU. Error bars reflect 15% error range.

and 3×10^5, respectively. As the colony increases to 3×10^6, the inhibited colony number reaches up to 50,000. These results suggest that the PHMGP-PA coating brings the antimicrobial ability into full play at a high colony of bacteria. Considering the large error in calculating the inhibited colony number at the colony of 3×10^7, it can be speculated that the measured antimicrobial performance of the PHMGP-PA coating at the colony of 3×10^6 approaches its true antimicrobial property in this test method.

Fig. 10 reports the antimicrobial properties of the fabric samples with different number of BL. At the colony of 3×10^6 CFU, 5 BL inhibits 39,000 colonies, and 10 BL inhibits 51,000 CFU. As the number of BL increases further to 20, the inhibited colony increases to 69,000. The inhibited colony number increases with the growth of BL at the colony of 3×10^6. Similar variation trends can also be observed at the colony of 3×10^5, 3×10^4 and 3×10^3. It suggests that the PHMGP-PA coating with more BLs possesses an enhanced antimicrobial ability, which is attributed to more antimicrobial PHMGP in the LBL coating. All these above results imply that the PHMGP-PA coating performs an efficient inhibiting effect on the growth of *E. coli*, in addition, it performs similar antimicrobial ability with the previous reported PHMGP-APP system with same assembly structure [40]. Even so, the PHMGP-PA multilayer assembled by the biodegradable materials without any obvious side effects can be more promising for the applications in household and healthcare items.

To further evaluate the antimicrobial ability of the PHMGP-PA coating, a quantitative determination were conducted on the antimicrobial properties of the fabric samples. In view of the coated samples were identified as dissolving type antimicrobial fabrics, we employed a modified AATCC test method 100–2004, in which two important pathogenic bacteria of human, gram-negative *E. coli* and gram-positive *S. aureus*, were selected as the representatives. As shown in Table 4, some bacteria die on the uncoated cotton as a result of the adhesion on the fabric surface. Because of the higher bacterial activity, the bacterial reduction of *S. aureus* is lower than that of *E. coli* for the uncoated fabric. With only 5 min contact time, the fabric coated with only 5 BLs can inhibit 100% *E. coli*. However, the 5 BL inactivates 55% *S. aureus*, and the bacterial reduction increases with the growth of bialyer number. As the BL number increases to 20, the inhibited *S. aureus* reaches up to 90%. When the contact time extends to 30 min, the coated fabrics can completely exterminate *S. aureus*. These results prove that the antimicrobial PHMGP possesses high antimicrobial activities on *E. coli* and *S. aureus* by damaging the cell membrane of bacteria and leaking the

Table 4
The antimicrobial properties of the fabric samples against *E. coli* and *S. aureus*. The error in the measured bacterial reduction is 15%.

Sample	Contact time (min)	Bacterial reduction (%) *E. coli*	*S. aureus*
Uncoated	5	14.29	25.00
	30	14.29	50.00
5 BL	5	100	55.00
	30	100	100
10 BL	5	100	75.00
	30	100	100
20 BL	5	100	90.00
	30	100	100

intracellular components [63–66]. What' more, *E. coli* is more susceptible to the antimicrobial PHMGP than *S. aureus*, which agrees well with the result from Kirby-Bauer test in our previous work [40].

4. Conclusions

An environmentally friendly intumescent flame retardant and antimicrobial LBL coating was successfully constructed on fabric by alternately depositing biodegradable ingredients of PHMGP and PA. In TGA, more char residues are left for the coated fabrics, due to the catalytic charring of PHMGP. In MCC test, the coated fabrics show small values of PHRR and THR than that of the uncoated, as a result of the inhibited release of volatile matters. In flammability test, no afterglow phenomenon appears and the wave structure is still maintained for the coated fabrics after burning. SEM images of the char residue reveal that many bubbles appear on the fibers for the 20 BL coated fabric, as a result of intumescent effect. Furthermore, the FTIR spectra of the char residues indicate that the PHMGP-PA coating performs flame retardant effect on cotton fabric by promoting the formation of intumescent char containing phosphorus-nitrogen aromatic structure during burning. Finally, the antimicrobial qualitative test results prove that the coated fabrics with more BLs possess higher antimicrobial performance, and the further quantitative tests results show the fabric coated with only 5 BLs can completely eliminate *E. coli* and *S. aureus* in 5 and 30 min, respectively.

Acknowledgment

We gratefully acknowledge the financial assistance from the National Natural Science Foundation of China (nos. 51303182 and 51402002).

References

[1] P.J.B. Wakelyn, N.R. French, A.D.D.P. Thibodeaux, Cotton Fiber Chemistry and Technology, Taylor & Francis Group, 2007.
[2] H.X. Yuan, W.Y. Xing, P. Zhang, L. Song, Y. Hu, Industrial & Engineering Chemistry Research 51 (2012) 5394.
[3] J. Vasiljevic, S. Hadzic, I. Jerman, L. Cerne, B. Tomsic, J. Medved, M. Godec, B. Orel, B. Simoncic, Polymer Degradation and Stability 98 (2013) 2602.
[4] W. Duan, A. Xie, Y. Shen, X. Wang, F. Wang, Y. Zhang, J. Li, Industrial & Engineering Chemistry Research 50 (2011) 4441.
[5] M.M.A.M. Montazer, The Journal of Physical Chemistry B 118 (2014) 1453.
[6] S.J.S. Chen, M. Xiong, J. Luo, J. Tang, Z. Ge, ACS Applied Materials & Interfaces 3 (2011) 1154.
[7] B.B. Hsu, A.M. Klibanov, Biomacromolecules 12 (2011) 6.
[8] G.A. Li, H. Wang, W.T. Zheng, R.K. Bai, Langmuir 26 (2010) 7529.
[9] Y.Y. Liu, J.H. Xin, C.H. Choi, Langmuir 28 (2012) 17426.
[10] A.H. Broderick, U. Manna, D.M. Lynn, Chemistry of Materials 24 (2012) 1786.
[11] Y. Yunjie, W. Chaoxia, W. Youjiang, Colloids and Surfaces A (Physicochemical and Engineering Aspects) 399 (2012) 92.
[12] Z.-D. Qi, T. Saito, Y. Fan, A. Isogai, Biomacromolecules 13 (2012) 553.
[13] Y. Zhao, Z.G. Xu, X.G. Wang, T. Lin, Langmuir 28 (2012) 6328.
[14] Q. Wang, P.J. Hauser, Carbohydrate Polymers 81 (2010) 491.
[15] R.K. Iler, Journal of Colloid and Interface Science 21 (1966) 569.
[16] G. Decher, J.D. Hong, Makromolekulare Chemie-Macromolecular Symposia 46 (1991) 321.
[17] Y.C. Li, J. Schulz, S. Mannen, C. Delhom, B. Condon, S. Chang, M. Zammarano, J.C. Grunlan, ACS Nano 4 (2010) 3325.
[18] W. Cai, J. Wu, C. Xi, A.J. Ashe 3rd, M.E. Meyerhoff, Biomaterials 32 (2011) 7774.
[19] J. Zhao, L.J. Song, J.H. Yin, W.H. Ming, Chemical Communications 49 (2013) 9191.
[20] Y.C. Li, J. Schulz, J.C. Grunlan, ACS Applied Materials & Interfaces 1 (2009) 2338.
[21] G.B. Huang, H.D. Liang, X. Wang, J.R. Gao, Industrial & Engineering Chemistry Research 51 (2012) 12299.
[22] F. Carosio, J. Alongi, G. Malucelli, Journal of Materials Chemistry 21 (2011) 10370.
[23] L. Yu-Chin, S. Mannen, J. Schulz, J.C. Grunlan, Journal of Materials Chemistry 21 (2011) 3060.
[24] G. Laufer, F. Carosio, R. Martinez, G. Camino, J.C. Grunlan, Journal of Colloid and Interface Science 356 (2011) 69.
[25] Y.-C. Li, S. Mannen, A.B. Morgan, S. Chang, Y.-H. Yang, B. Condon, J.C. Grunlan, Advanced Materials 23 (2011) 3926.
[26] J. Alongi, Z. Han, S. Bourbigot, Progress in Polymer Science (2015).
[27] F. Fang, X. Zhang, Y. Meng, Z. Gu, C. Bao, X. Ding, S. Li, X. Chen, X. Tian, Surface and Coatings Technology 262 (2015) 9.
[28] T. Zhang, H.Q. Yan, L.L. Wang, Z.P. Fang, Industrial & Engineering Chemistry Research 52 (2013) 6138.
[29] A.A. Cain, S. Murray, K.M. Holder, C.R. Nolen, J.C. Grunlan, Macromolecular Materials and Engineering 299 (2014) 1180.
[30] F. Carosio, G. Fontaine, J. Alongi, S. Bourbigot, ACS Applied Materials & Interfaces 7 (2015) 12158.
[31] F. Carosio, J. Alongi, G. Malucelli, Carbohydrate Polymers 88 (2012) 1460.
[32] G. Laufer, C. Kirkland, A.B. Morgan, J.C. Grunlan, Biomacromolecules 13 (2012) 2843.
[33] F. Carosio, A. Di Blasio, J. Alongi, G. Malucelli, Polymer 54 (2013) 5148.
[34] K. Apaydin, A. Laachachi, V. Ball, M. Jimenez, S. Bourbigot, V. Toniazzo, D. Ruch, Polymer Degradation and Stability 106 (2014) 158.
[35] H.F. Pan, L. Song, L.Y. Ma, Y. Pan, K.M. Liew, Y. Hu, Cellulose 21 (2014) 2995.
[36] L.L. Wang, T. Zhang, H.Q. Yan, M. Peng, Z.P. Fang, Y. Li, W. Hao, Chinese Journal of Polymer Science 32 (2014) 305.
[37] H. Pan, W. Wang, Y. Pan, L. Song, Y. Hu, K.M. Liew, Carbohydrate Polymers 115 (2015) 516.
[38] A. Hebeish, M.E. El-Naggar, M.M.G. Fouda, M.A. Ramadan, S.S. Al-Deyab, M.H. El-Rafie, Carbohydrate Polymers 86 (2011) 936.
[39] A. Hebeish, F.A. Abdel-Mohdy, M.M.G. Fouda, Z. Elsaid, S. Essam, G.H. Tammam, E.A. Drees, Carbohydrate Polymers 86 (2011) 1684.
[40] F. Fang, D. Xiao, X. Zhang, Y. Meng, C. Cheng, C. Bao, X. Ding, H. Cao, X. Tian, Surface and Coatings Technology 276 (2015) 726.
[41] J. Alongi, R.A. Carletto, A. Di Blasio, F. Cuttica, F. Carosio, F. Bosco, G. Malucelli, Carbohydrate Polymers 96 (2013) 296.
[42] F. Carosio, A. Di Blasio, F. Cuttica, J. Alongi, G. Malucelli, Industrial & Engineering Chemistry Research 53 (2014) 3917.
[43] O. Kukharenko, J.-F. Bardeau, I. Zaets, L. Ovcharenko, O. Tarasyuk, S. Porhyn, I. Mischenko, A. Vovk, S. Rogalsky, N. Kozyrovska, European Polymer Journal 60 (2014) 247.
[44] Y.K. Mathurin, R. Koffi-Nevry, S.T. Guehi, K. Tano, M.K. Oule, Journal of Food Protection 75 (2012) 1167.
[45] G. Muller, A. Kramer, Journal of Orthopaedic Research 23 (2005) 127.
[46] B.R. Kim, J.E. Anderson, S.A. Mueller, W.A. Gaines, A.M. Kendall, Water Research 36 (2002) 4433.
[47] T. Buchberger, M. Himmelsbach, W. Buchberger, Journal of Chromatography A 1318 (2013) 22.
[48] E.M. Zactiti, T.G. Kieckbusch, Journal of Food Engineering 77 (2006) 462.
[49] H. Madziva, K. Kailasapathy, M. Phillips, Lwt-Food Science and Technology 39 (2006) 146.
[50] K. Norajit, K.M. Kim, G.H. Ryu, Journal of Food Engineering 98 (2010) 377.
[51] P. Matricardi, M. Pontoriero, T. Coviello, M.A. Casadei, F. Alhaique, Biomacromolecules 9 (2008) 2014.
[52] K.Y. Lee, D.J. Mooney, Progress in Polymer Science 37 (2012) 106.
[53] S. Dhat, S.R. Naik, A. Agharkar, P. Kulkarni, Journal of Pharmacy Research 2 (2009) 1098.
[54] J. Zhang, Q. Ji, X. Shen, Y. Xia, L. Tan, Q. Kong, Polymer Degradation and Stability 96 (2011) 936.
[55] Y. Liu, J. Zhao, C. Zhang, H. Ji, P. Zhu, Journal of Macromolecular Science Part B: Physics 53 (2014) 1074.
[56] C. Chung, M. Lee, E. Choe, Carbohydrate Polymers 58 (2004) 417.
[57] G. Lawrie, I. Keen, B. Drew, A. Chandler-Temple, L. Rintoul, P. Fredericks, L. Grondahl, Biomacromolecules 8 (2007) 2533.
[58] Y.M. Zhang, J.M. Jiang, Y.M. Chen, Polymer 40 (1999) 6189.
[59] J. Alongi, C. Colleoni, G. Rosace, G. Malucelli, Polymer Degradation and Stability 99 (2014) 92.
[60] Y.N. Phang, S.Y. Chee, C.O. Lee, Y.L. Teh, Polymer Degradation and Stability 96 (2011) 1653.
[61] J. Zhan, L. Song, S.B. Nie, Y.A. Hu, Polymer Degradation and Stability 94 (2009) 291.
[62] Y. Liu, J. Yi, X. Cai, Journal of Thermal Analysis and Calorimetry 107 (2011) 1191.
[63] G. McDonnell, A.D. Russell, Clinical Microbiology Reviews 12 (1999) 147.
[64] P. Gilbert, L.E. Moore, Journal of Applied Microbiology 99 (2005) 703.
[65] Z.X. Zhou, D.F. Wei, Y. Guan, A.N. Zheng, J.J. Zhong, Journal of Applied Microbiology 108 (2010) 898.
[66] L. Timofeeva, N. Kleshcheva, Applied Microbiology and Biotechnology 89 (2011) 475.